Molecular Neurobiology (2019) 56:3175–3192
https://doi.org/10.1007/s12035-018-1292-5

An Antagonistic Axon-Dendrite Interplay Enables Efficient Neuronal Repair in the Adult Zebrafish Central Nervous System

An Beckers[1] · Annelies Van Dyck[1] · Ilse Bollaerts[1] · Jessie Van houcke[1] · Evy Lefevere[1] · Lien Andries[1] · Jessica Agostinone[2] · Inge Van Hove[1] · Adriana Di Polo[2] · Kim Lemmens[1] · Lieve Moons[1]

Received: 30 March 2018 / Accepted: 31 July 2018 / Published online: 13 August 2018
© Springer Science+Business Media, LLC, part of Springer Nature 2018

Abstract

Neural insults and neurodegenerative diseases typically result in permanent functional deficits, making the identification of novel pro-regenerative molecules and mechanisms a primary research topic. Nowadays, neuroregenerative research largely focuses on improving axonal regrowth, leaving the regenerative properties of dendrites largely unstudied. Moreover, whereas developmental studies indicate a strict temporal separation of axogenesis and dendritogenesis and thus suggest a potential interdependency of axonal and dendritic outgrowth, a possible axon-dendrite interaction during regeneration remains unexplored. To unravel the inherent dendritic response of vertebrate neurons undergoing successful axonal regeneration, regeneration-competent adult zebrafish of either sex, subjected to optic nerve crush (ONC), were used. A longitudinal study in which retinal ganglion cell (RGC) dendritic remodeling and axonal regrowth were assessed side-by-side after ONC, revealed that—as during development—RGC axogenesis precedes dendritogenesis during central nervous system (CNS) repair. Moreover, dendrites majorly shrank before the start of axonal regrowth and were only triggered to regrow upon RGC target contact initiation, altogether suggestive for a counteractive interplay between axons and dendrites after neuronal injury. Strikingly, both retinal mechanistic target of rapamycin (mTOR) and broad-spectrum matrix metalloproteinase (MMP) inhibition after ONC consecutively inhibited RGC synapto-dendritic deterioration and axonal regrowth, thus invigorating an antagonistic interplay wherein mature dendrites restrain axonal regrowth. Altogether, this work launches dendritic shrinkage as a prerequisite for efficient axonal regrowth of adult vertebrate neurons, and indicates that molecular/mechanistic analysis of dendritic responses after damage might represent a powerful target-discovery platform for neural repair.

Keywords Optic nerve crush · Dendritic remodeling · Axonal regeneration · mTOR and MMP inhibitor studies · Retina · Zebrafish

Introduction

Defects in dendritic arborization and connectivity represent one of the first stages of mammalian central nervous system (CNS) neurodegeneration. Also glaucomatous optic neuropathies are characterized by early retinal synapse loss, retinal ganglion cell (RGC) dendritic shrinkage, and a reduced dendritic complexity, which likely precede irreversible structural damage to the optic nerve and RGC death [1, 2]. Recent strategies aiming to preserve RGC functioning therefore strive to maintain their dendritic and synaptic stability [3]. Unfortunately, as the majority of patients diagnosed with a glaucomatous optic neuropathy already suffer from severe optic nerve and RGC damage, functional neuronal network repair not only requires neuroprotection but also axonal regeneration of harmed RGCs. Over the years, multifactorial strategies able to boost the regenerative potential of the mammalian CNS have been identified by investigating both spontaneous (e.g., zebrafish) and experimentally induced (e.g., rodents) optic nerve regeneration within the visual system, which is still one of the most powerful model systems available to study axonal regrowth [4, 5]. Dendrites, however, despite being an equal essential component of the neuronal circuitry, have been

Kim Lemmens and Lieve Moons contributed equally to this work.

✉ Lieve Moons
lieve.moons@kuleuven.be

[1] Neural Circuit Development and Regeneration Research Group, Department of Biology, KU Leuven, Naamsestraat 61, box 2464, 3000 Leuven, Belgium

[2] Department of Neuroscience and Centre de recherche du Centre hospitalier de l'Université de Montréal (CRCHUM), University of Montréal, Montréal, QC, Canada

overlooked for decades in regenerative research. Indeed, apart from a few publications reporting diverse effects on RGC dendritic structure in peripheral nerve-optic nerve grafting experiments [6, 7], studies investigating dendritic remodeling in the regenerating vertebrate CNS remain scarce.

In contrast to the injured adult CNS, dendritic remodeling is well-studied during development of the vertebrate retinofugal system, in which there is a distinct temporal window for RGC axon growth versus dendritic expansion. First, newly born RGCs initiate an axon that extends into the optic nerve to reach its target cells in the brain. Either just before or upon target contact initiation, RGC dendrites emerge and grow into the inner plexiform layer (IPL) to connect with other retinal neurons [8, 9]. This orderly process suggests that the timing of axon versus dendrite outgrowth is distinct and tightly regulated during development. Whether neurons recapitulate this developmental sequence during repair in the damaged adult CNS is not completely understood.

The adult teleost *Danio rerio* is a well-established and powerful model system for the molecular and mechanistic study of neural regeneration, since it possesses phylogenetically conserved and robust neuroregenerative capacities in both brain and retina [10–16]. Moreover, it has also proven to be a perfect model to investigate the underlying mechanisms of axonal regeneration [5, 15] and will therefore be used in this study to examine a possible interplay between dendrite remodeling and axon regrowth in regeneration-competent adult neurons (RGCs) subjected to axonal injury. As such, to characterize the inherent response of dendrites during successful spontaneous RGC axonal regeneration, we performed IPL thickness measurements and spatial/temporal expression analysis of dendritic (Map2) and synaptic (Sv2, Psd-95, Znp-1) markers in the fish retina during different phases of RGC axonal regeneration, i.e., during (1) injury response, (2) axonal regrowth, (3) optic tectum reinnervation, and (4) primary target contact restoration in the brain. Notably, using this approach, we reveal that dendritic shrinkage is evoked prior to axonal regrowth and that injured regeneration-competent neurons are programmed to copy the developmental order of neurite growth, in which axogenesis is prior to dendritogenesis [9, 17].

Invigorated by the recently reported existence of invertebrate bimodal controllers, which repress axonal growth during dendritogenesis and vice versa [18], we hypothesized that the observed sequential organization of neurite collapsing and regrowth in crushed adult zebrafish RGCs might indicate an antagonistic interplay between vertebrate RGC axons and dendrites upon injury, wherein disturbed dendritic pruning could repress axonal regrowth. To evidence this hypothesis, we interfered with retinal mechanistic target of rapamycin (mTOR) and matrix metalloproteinase (MMP) functioning upon optic nerve crush (ONC) in adult zebrafish. Both, mTOR, a serine/threonine kinase of the phosphoinositide 3-kinase (PI3K)-related kinase family, and MMPs, Zn^{2+}-dependent endopeptidases of the metzincin family, have been suggested as key players in zebrafish and mammalian RGC axonal regeneration [19–22]. Importantly, both molecules are also known regulators of synaptogenesis and of neuronal dendrite development, stabilization, and (activity-dependent) dendritic remodeling [23–26]. Intriguingly, we now show that rapamycin-mediated inhibition of retinal mTOR activation in adult zebrafish after ONC prevents dendrites from retracting and, later on, results in a diminished optic tectum reinnervation by regrowing RGC axons. We recently reported that lowering retinal MMP activity in vivo greatly reduces RGC axonal regrowth in adult zebrafish subjected to ONC [21]. Importantly, and conform with the mTOR data, we here provide evidence that the aberrant effect on RGC axonal regeneration seen upon local broad-spectrum MMP inhibition could be—at least partly—attributable to its counteracting effect on retinal dendritic retraction and synaptic deterioration.

Altogether, these data provide first insights into a potential antagonistic interplay between vertebrate RGC axons and dendrites after ONC, wherein disturbed dendritic pruning might repress axonal regrowth.

Results

Characterization of Retinal Dendritic Remodeling After Optic Nerve Injury

In a first attempt to assess retinal dendritic remodeling after ONC, the ratio IPL/total retinal thickness was analyzed on H&E-stained retinal sections of eyes isolated at baseline (naive) and at 1, 4, 7, 10, 14, and 18 days post-injury (dpi). Representative images of the central retina are shown at preeminent time points in Fig. 1. At both 4 and 7 dpi, a significant reduction in relative IPL thickness of approximately 20% was observed in the central retina in comparison to naive fish (Fig. 1, $n = 3–6$, one-way ANOVA, $F_{(6,\ 24)} = 4.94$, $p = 0.001$, Dunnet post-hoc test, p (Naive vs. 4 dpi) = 0.014, p (Naive vs. 7 dpi) = 0.012). Notably, IPL thickness had again increased by 10 dpi relative to 4 and 7 dpi, and reapproached baseline values from 14 dpi onwards, altogether suggestive of the occurrence of dendritic remodeling after optic nerve injury.

Optic Nerve Injury Induces Subsequent Loss and Repair of Synaptic Connectivity in the Adult Zebrafish Retina

As the maintenance of synaptic input is important to assure dendritic stability [27], the spatiotemporal expression pattern of Synaptic vesicle protein 2 (Sv2), a validated marker of synaptic vesicles in the IPL and outer plexiform layer (OPL) of fish retina [28, 29], was determined using Western blotting (WB) on retinal lysates harvested at baseline (naive), 6 h post-injury (hpi), and 1, 4, 7, 10, 14, and 18 dpi. Total protein staining was used as protein loading control and data were plotted as a relative percentage to baseline level in naive fish, which was set

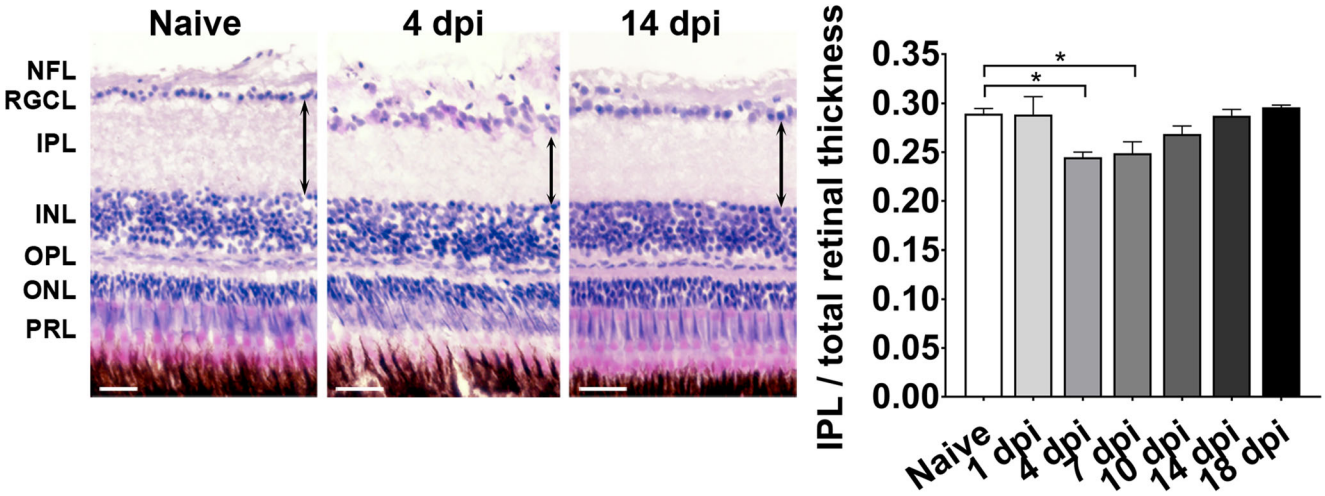

Fig. 1 IPL thinning and restoration suggests dendritic shrinkage and subsequent regrowth after ONC in zebrafish**.** Representative images of H&E-stained retinal sections and quantitative analysis of IPL/total retinal thickness show a significant reduction in IPL thickness in retinas of fish at 4 and 7 dpi as opposed to naive retinas. Baseline IPL/total retinal thickness values are regained at 2 weeks after ONC. Scale bar = 20 μm. Data represent mean ± SEM. *NFL* nerve fiber layer, *RGCL* retinal ganglion cell layer, *IPL* inner plexiform layer, *INL* inner nuclear layer, *OPL* outer plexiform layer, *ONL* outer nuclear layer, *PRL* photoreceptor layer

as 100%. A ~25% decrease in Sv2 expression (95 kDa) was already perceptible at 6 hpi and became significant by 4 dpi as compared to naive fish (Fig. 2a, $n = 3–6$, Kruskal-Wallis, Df = 6, $H = 11{,}67$, $p = 0.039$, Dunnet post-hoc test, p (Naive vs. 4 dpi) = 0.019). Recovery of Sv2 expression was induced from 10 dpi onwards and again reached control levels by 14 dpi.

To strengthen this observation more specifically for RGC retinal synapses, immunostaining for the post-synaptic density protein 95 (Psd-95), an excitatory post-synaptic density marker known to label synapses on RGC dendrites in both fish and mammals [1, 30], was performed on retinal sections of naive and crushed fish at various days post-injury. Representative images in Fig. 2b clearly show abundant expression of Psd-95 in the IPL of naive fish and a subsequent reduction in Psd-95 signal shortly after ONC, at 1 dpi. The Psd-95 signal in the IPL diminished even further at 4 (and 7, data not shown) dpi with respect to naive retinas (Fig. 2b). In accordance with the Sv2 WB data, these findings indicate a rapid reduction in RGC post-synaptic connectivity after ONC. Of note, no reduction in Psd-95 signal in the IPL was observed at 6 hpi (data not shown), in contrast to the Sv2 WB data, likely because immunohistochemistry is less quantitative and not as sensitive as WB to detect minor changes in protein levels. Notably, Psd-95 staining could again be observed in the IPL from 10 dpi onwards, which likely represents the initiation of synapse formation between RGC dendrites and bipolar cell neurites as the PSD-95 family is thought to regulate synapse assembly and function [30]. This generation of novel synapses was seemingly completed between 14 and 18 days post-ONC as the Psd-95 staining pattern then again resembled baseline conditions. Confirmatory, also for Znp-1, a known marker of bipolar/amacrine cell pre-synaptic nerve terminals in the IPL of the vertebrate retina, an identical temporal decrease in signal could be observed (Fig. 2b) [31, 32]. Taken together, these data are indicative of early synaptic degeneration and subsequent synaptogenesis in the inner retina of adult zebrafish, subjected to optic nerve injury.

Optic Nerve Injury Triggers Dendritic Remodeling in the Adult Zebrafish Retina

To obtain direct insights into retinal dendritic changes after ONC, the spatiotemporal expression pattern of microtubule-associated protein 2 (Map2) was first characterized via WB on retinal lysates harvested at baseline (naive) and at 6 hpi, 1, 4, 7, 10, 14, and 18 dpi. Map2 is a validated marker for (IPL) dendrites and is known to be essential for dendritic stabilization and outgrowth in vertebrates [33–36]. A decrease in Map2 (280 kDa) levels was already observed 6 h after damage and became significant at 1 dpi. Map2 levels eventually augmented again around 10 dpi and reattained control levels by 2 weeks after ONC (Fig. 2a, $n = 6–18$, one-way ANOVA, $F_{(5, 45)} = 3.940$, $p = 0.005$, Dunnet post-hoc test, p (Naive vs. 1 dpi) = 0.027, p (Naive vs. 4 dpi) = 0.016, p (Naive vs. 7 dpi) = 0.012). An immunostaining for Map2 on retinal sections confirmed these results. Indeed, the clear Map2 dendritic labeling that was visible in naive conditions already decreased at 1 dpi, but not at 6 hpi (data not shown), and reached minimal expression at 4 dpi. Hereafter, the Map2 immunopositive area increased again from 10 dpi onwards and reached baseline expression 4 days later (Fig. 2b). As Map2 prevents microtubule depolymerization and thus preserves dendritic morphology, the reduction of retinal Map2 expression suggests a profound degeneration/collapse of dendrites in the retina immediately after ONC [34, 37, 38]. Likewise, the subsequent gradual restoration of Map2 protein towards baseline values by 14

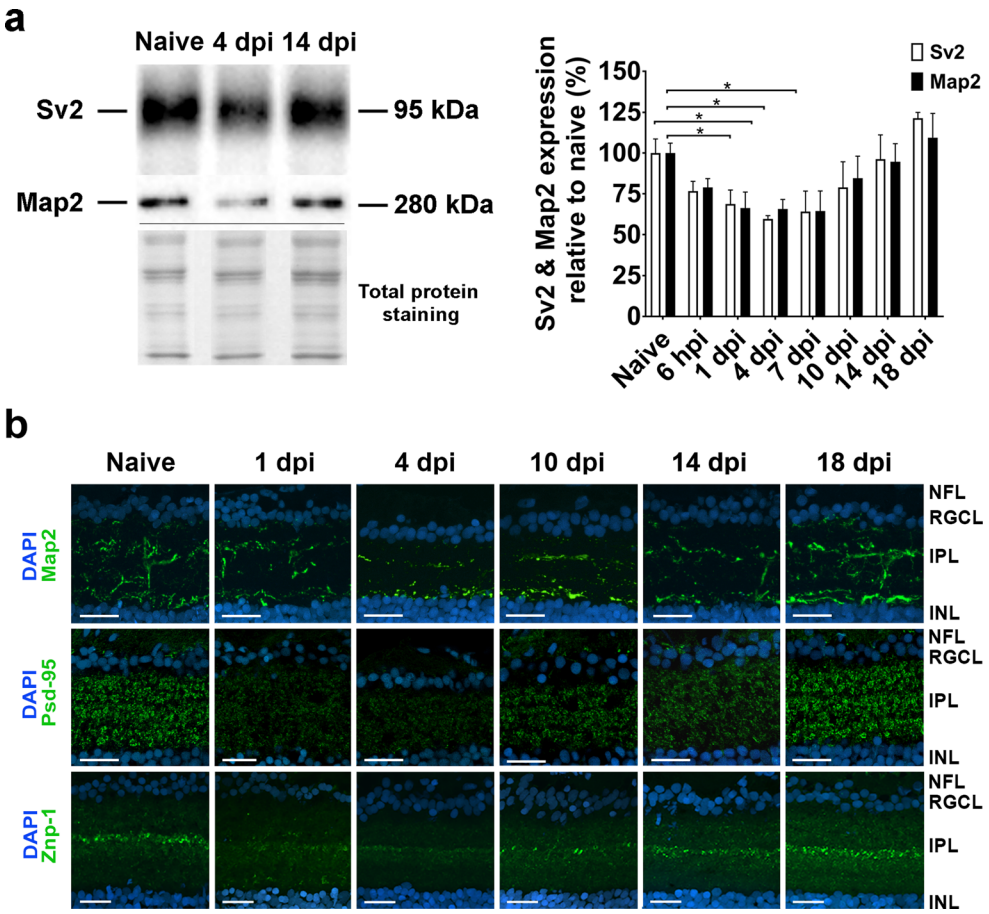

Fig. 2 ONC in zebrafish triggers immediate retinal synaptic deterioration and dendritic pruning, followed by dendritic regrowth and synaptic repair. **a** Representative picture and bar graph showing WB analysis data for Sv2 and Map2 expression in retinal extracts after ONC, each plotted as a relative percentage to the expression in naive fish retinas. Both Sv2 and Map2 levels decreased from 6 hpi onwards and started to increase again around 10 dpi to reattain control values at 14 dpi, thus pointing to consecutive synaptic/dendritic degeneration and regrowth. Swift membrane total protein staining served as loading control. Data represent mean ± SEM. **b** Immunostainings for Psd-95 and Znp-1 showed a decline in fluorescent signal in the IPL by 1 dpi, indicating post-synaptic and amacrine/bipolar cell pre-synaptic terminal degeneration, which goes hand in hand with dendritic shrinkage as also Map2 immunopositivity is decreased from 1 dpi on. Of note, no decline in fluorescent signal for Psd-95, Znp-1, or Map2 was visible at 6 hpi. From 10 dpi onwards, Psd-95, Znp-1, and Map2 signals start to reappear, pointing toward the restoration of dendritic trees and the generation of novel synaptic contacts between RGCs and amacrine/bipolar cells. Between 14 and 18 dpi, baseline levels are regained, indicating near completion of dendritic regrowth and retinal synaptogenesis. DAPI (blue) was used as nuclear counterstain. Scale bar = 20 μm. *NFL* nerve fiber layer, *RGCL* retinal ganglion cell layer, *IPL* inner plexiform layer, *INL* inner nuclear layer

dpi marks the graduated return of stable and mature RGC dendrites (Fig. 2b).

Characterization of RGC Axonal Regeneration After Optic Nerve Injury

To diversify dendritic alterations in relation to the different phases of axonal regeneration and in order to map the temporal occurrence of the axonal growth response in detail, we next determined the injury response, axonal regrowth, optic tectum reinnervation, and target contact phases after optic nerve injury. For this, retinal mRNA levels of growth-associated protein 43 (*gap-43)*—a validated marker for axonal growth—were determined at baseline, 6 hpi, 1 and 4 dpi. *Gap-43* showed no significant induction at the earliest time points after ONC (6 hpi and 1 dpi), but was highly up-regulated by 4 dpi as compared to baseline (Fig. 3a, $n = 4–5$, one-way ANOVA, $F_{(4, 17)} = 29{,}085$, $p < 0.0001$, Dunnet post-hoc test, p (Naive vs. 4 dpi) < 0.0001). This highly corresponds with our previously determined retinal Gap-43 expression pattern at the protein level, in which we also observed no detectable gap-43 protein upregulation until 1 dpi, and a peak in expression at 4 dpi [21]. In accordance with previous publications, these data allow us to define the injury response phase from 0 to 1 dpi, in which there is no significant induction of *gap-43* expression [21, 39]. The small, though non-significant rise in *gap-43* mRNA expression seen at 1 dpi likely indicates the start of the axonal regrowth phase, in which a small number of pioneering neurons already starts to regrow their axons. As previously described, axonal regrowth then starts around 1 dpi and is maximally ongoing at 4 dpi, with

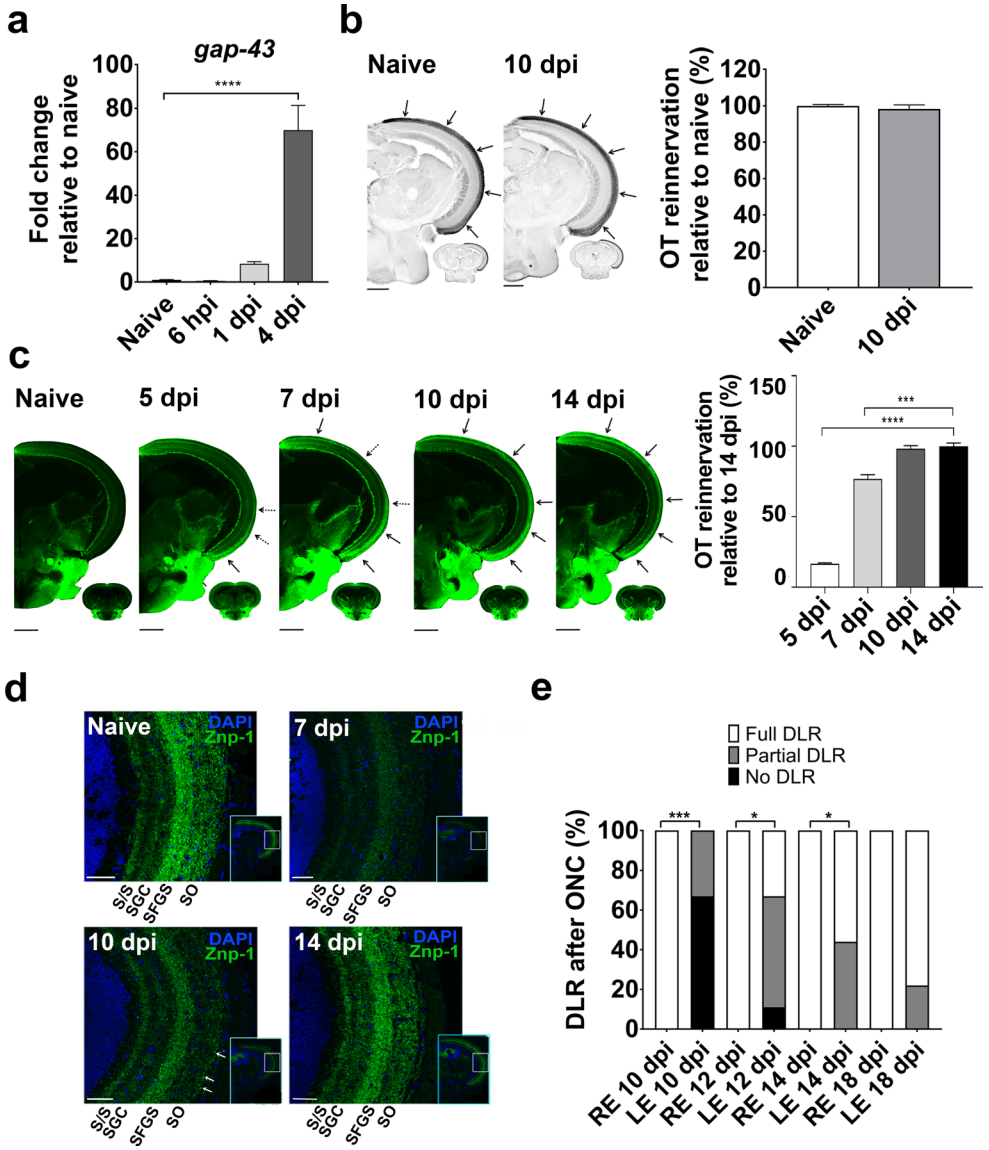

Fig. 3 Mapping of RGC axonal regrowth after ONC in adult zebrafish. **a** RT-qPCR for retinal *gap-43* reveals a rise in gene expression from 1 dpi onwards, which becomes statistically significant at 4 dpi, compared to baseline levels. Data represent mean fold change values relative to naive ± SEM. **b** Microscopic images of biocytin-labeled brain sections of naive and injured fish at 10 dpi visualizing innervation of the SO and SFGS in the contralateral optic tectum by RGC axons. Arrows indicate RGC terminals entering the optic tectum. Quantification of the area covered by RGC axons in the optic tectum of 10 dpi fish, relative to naive fish, confirms that tectal reinnervation is completed at 10 dpi. Scale bar = 200 µm. Data represent mean ± SEM. **c** Analysis of Gap-43^{+} area in Tg(*fGap-43:GFP*) fish after ONC indicates that the first axons arrive at 5 dpi. The optic tectum is reinnervated for 70% and 100% at 7 and 10/14 days, respectively. Data represent mean ± SEM. **d** Representative immunostainings for Znp-1 on transverse optic tectum sections at various stages post-injury show Znp-1 downregulation in the SO and SFGS at 7 and 10 dpi relative to naive fish. Znp-1 signal reapproached baseline levels in the SO and SFGS of the optic tectum at 14 dpi, indicative of synaptic repair between RGC terminals and their primary neuronal targets in the brain. DAPI (blue) was used as nuclear counterstain. White arrows indicate newly formed synapses in the SO. Scale bar = 20 µm. **e** Complete, mild, and absence of body axis tilting in response to a dorsal to ventral moving light influx, was assessed for both eyes (control right eye: RE, crushed left eye: LE) and denoted as a full, partial, and no DLR, respectively. The degree of body axis tilting remained significantly different between the control right and crushed left eye until 14 dpi. At 18 dpi, the DLR of the left crushed eye was restored as compared to that of the right control eye. Graph represents semi-quantitative scoring of DLRs. *OT* optic tectum

retinal mRNA and protein expression of Gap-43 peaking at that moment (Fig. 3a, [21, 40]).

We previously showed—by means of analysis of optic tectum reinnervation via anterograde biocytin tracing—that the first regrowing RGC axons re-enter the optic tectum at 5 dpi and that already ~70% of the optic tectum is reinnervated at 7 dpi, as compared to the RGC innervated tectal area in naive fish, demonstrating that optic tectum innervation by RGC axons is fully ongoing at that time [21, 41]. Using the similar semi-quantitative analysis of tectal reinnervation at later time

points post-injury, we now reveal that optic tectum reinnervation is fully completed by 10 dpi (Fig. 3b, $n = 4$, two-tailed t test, $t(6) = 0.704$, $p = 0.508$). Next, these data were confirmed using Tg(*fGap-43*:*GFP*) zebrafish [42] (Fig. 3c, $n = 3$, one-way ANOVA, $F_{(3, 8)} = 307{,}289$, $p < 0.0001$, Dunnet post-hoc test, p (14 dpi vs. 5 dpi) < 0.0001, p (14 dpi vs. 7 dpi) = 0.0002). Indeed, Gap-43 expression is visible in the optic tectum from 4 to 5 days after ONC, visualizing the pioneering axons. Two days later, already 70% of the tectal area was Gap-43 positive, as compared to the labeled area 14 days after ONC, a time point at which previous biocytin tracing experiments indicated that optic tectum reinnervation is already fully completed. Similar as shown with biocytin tracing, optic tectum reinnervation is already completed at 10 dpi.

Furthermore, immunostainings for Znp-1 (anti-synaptotagmin 2) were performed on optic tectum sections of naive fish and fish at different time points post-ONC to assess the presence of RGC pre-synaptic termini in the tectum during the course of retinotectal regeneration, and thus to define the start of the target contact reinnervation phase. As depicted in Fig. 3d, naive fish show abundant staining for RGC terminals in the stratum opticum (SO) and stratum fibrosum et griseum superficiale (SFGS), the primary RGC synaptic contact layers, and to a lesser extent in the stratum griseum centrale (SGC) and a projection zone (S/S) between the stratum album centrale (SAC) and stratum periventriculare (SPV), both innervated by a small subset of RGCs [43]. The Znp-1 signal decreased after injury to reach very low expression levels at 7 dpi, which then gradually re-emerged at 10 dpi, marking an initiation of RGC target contact restoration near the time point at which tectal reinnervation is completed. At 2 weeks post-injury, Znp-1 staining intensity returned to baseline levels in all layers, thus showing extensive repair of RGC synaptic contacts with their neuronal targets in the optic tectum between 10 and 14 dpi (Fig. 3d).

Next, to analyze functional recovery of primary vision, dorsal light reflex (DLR) testing was applied in adult zebrafish after optic nerve lesion [44, 45]. Fish were subjected to a DLR test at four consecutive time points after ONC, using the right uncrushed eye as a positive control. At 10 dpi, most (67%) fish were unable to perform a DLR and only 33% of the fish showed a partial DLR (partial tilting of the body axis). Yet, 4 days later, all fish could at least accomplish a partial (44%) or even complete (56%) DLR response (Fig. 3e, $n = 9$, Chi-square test, Df = 2, p (RE 10 dpi vs. LE 10 dpi) = 0.001, p (RE 12 dpi vs. LE 12 dpi) = 0.011, p (RE 14 dpi vs. LE 14 dpi) = 0.023, p (RE 18 dpi vs. LE 18 dpi) = 0.133). In accordance with the Znp-1 data, these results suggest a massive RGC target reconnection in the optic tectum at 2 weeks post-injury. By 18 dpi, DLR responses of the left crushed and right control eye were similar in all fish, indicating a fully restored DLR and thus complete recovery of primary visual function (Fig. 3e) [46].

A Distinct and Time-Restricted Dendritic and Axonal Growth Response During RGC Regeneration

To obtain detailed insight into the time course and extend of dendritic remodeling versus axonal regrowth after ONC, the rate of the growth responses of both processes were estimated based on gathered experimental data (Figs. 1, 2, and 3) and were plotted in relation to time. The drawings below visualize a neuron undergoing dendritic shrinkage and axonal regeneration after ONC in relation to time. The orange line in this figure depicts the dendritic growth response curve and indicates that, similar as in mammals, optic nerve damage rapidly reduces retinal synaptic density and triggers dendritic shrinkage immediately after ONC. This results in a negative growth response that reaches its minimum at 4 dpi (cfr. maximum decline in IPL thickness and Sv2, Psd-95, Znp-1, and Map2 expression, Figs. 1 and 2), and stays that way until about 10 dpi. Notably, the observed dendrite retraction is followed by a clear dendrite outgrowth response, increasing from 10 to 14 dpi, a time period during which retinal synapse and dendrite integrity is fully regained (cfr. IPL thickness and Sv2, Psd-95, Znp-1, and Map2 expression rereach control values, Figs. 1 and 2).

The axonal growth response curve, pictured by a blue line in the schematic time-course overview (Fig. 4), reveals that axon outgrowth only starts around 1 dpi (cfr. slight increase in *gap-43* expression in Fig. 3a), thus after the start of dendritic retraction, and steadily rises until 4 dpi (cfr. peak in Gap-43 expression in Fig. 3a and [21]), exactly when the dendritic growth response is at its minimum. Hereafter, optic tectum reinnervation starts, resulting in 70% tectum reinnervation at 7 dpi (Fig. 3b). The axonal growth response then peaks at 7 dpi, and declines after this to reach zero outgrowth around 10 dpi (cfr. completion of tectal reinnervation, Fig. 3b, c), simultaneous with the initiation of dendritic regrowth. Finally, the completed tectal innervation is followed by RGC synaptic target contact initiation in the brain and primary visual recovery (cfr. increase in Znp-1 signal in the optic tectum from 10 dpi onwards, Fig. 3d and restoration of DLR by 18 dpi, Fig. 3e). Our data thus reveal that injured adult regeneration-competent neurons possess a remarkable synaptic/dendritic remodeling potential, and that they are programmed to recapitulate developmental neurite outgrowth, wherein axogenesis precedes dendritogenesis [9, 17]. Remarkably, and potentially even more intriguing than these findings, is the meticulous orchestration of the axonal and dendrite growth response over time. Indeed, both responses nicely complement each other. ONC first evokes clear synaptic degeneration and RGC dendritic shrinkage in the inner retina before RGC axonal regrowth is initiated. Thereafter, dendrites are only triggered to regrow during the transition from RGC optic tectum innervation to synaptic target contact repair in the brain. Overall, our data are

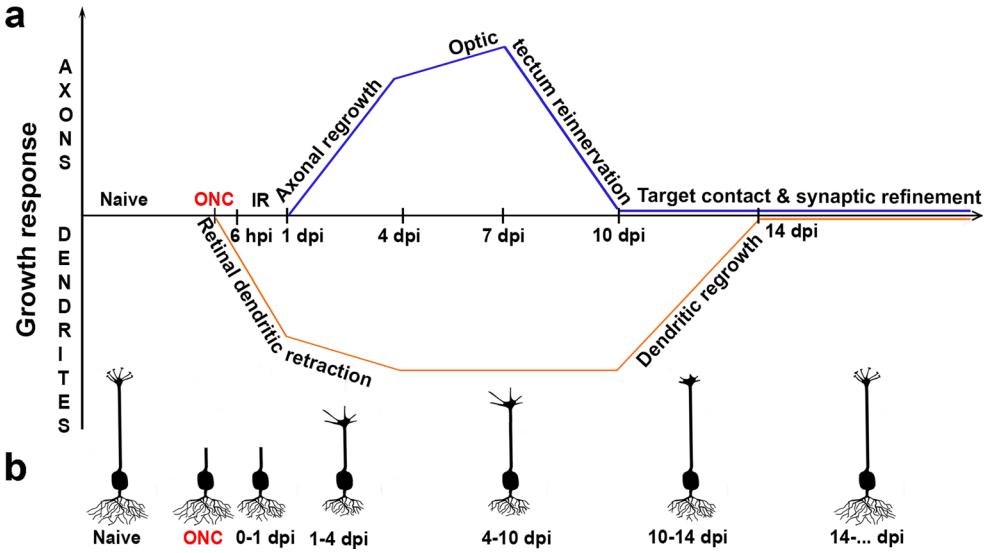

Fig. 4 Schematic representation of RGC axonal regeneration and dendritic remodeling in relation to the growth response reveals a sequential progress of these two processes after ONC. **a** The graph depicts the estimated dendritic (orange) and axonal (blue) growth responses, in which descending and ascending lines respectively project a negative and positive growth response. During the injury response phase (0–1 dpi), the dendritic growth response commences to diminish, as the dendrites immediately start to retract after injury. The axonal growth response initiates at 1 dpi and rapidly increases to peak at 7 dpi. The decline in growth response from 7 to 10 dpi denotes the last phase of optic tectum reinnervation, during which the dendritic growth response is retained at an absolute minimum. At the end of tectal innervation/onset of RGC target contact restoration, i.e., around 10 dpi, the dendritic growth response shifts to a regrowth modus which increases to complete dendritic regeneration by 14 dpi. **b** The schematic drawings below the graph clarify the de/regenerative status of the RGC axons and dendrites at consecutive time points after ONC. Briefly, ONC first triggers RGC dendritic shrinkage during the injury response phase (0–1 dpi). Dendritic retraction continues to a maximum during massive axonal regrowth occurring between 1 and 4 dpi. Dendritic morphology remains reduced during RGC tectal reinnervation (4–10 dpi). Parallel to initiation of RGC target contact repair in the brain (10 dpi), dendrites are triggered to regrow and establish novel synaptic connections (10–14 dpi), ultimately resulting in primary visual repair within 3 weeks after ONC. *IR* injury response

suggestive of an antagonistic and hence interdependent interplay between RGC axonal regrowth and dendritic remodeling during CNS regeneration.

Retinal mTOR Inhibition Prevents Early Retinal Synaptic/Dendritic Degeneration and Disturbs RGC Axonal Regrowth After Optic Nerve Injury

Regarding the established role of mTOR as keeper of cellular homeostasis, its capacity to promote vertebrate optic nerve regeneration, and its alleged contribution to dendrite dynamics, we postulated that interfering with retinal mTOR activity in adult zebrafish after ONC might provide primary insights into this potential dendrite-axon interrelatedness and its importance in successful neuronal regeneration. Diekmann et al. [22] already described that a rise in mTOR activation (mTORC1 in particular) was detected in the retinal ganglion cell layer (RGCL) of crushed zebrafish at 1 dpi that peaked 1 day later and was completely resolved by 4 dpi [22]. As dendritic remodeling immediately starts after ONC, and we wanted to affect this process via mTOR inhibition, we first characterized early mTORC1 activity at 6 hpi. For this, a triple staining for phosphorylated S6 (pS6, mTORC1 activity marker), acetylated-tubulin (AcT) to count RGCs, and choline acetyltransferase (CHAT, amacrine cells) was performed on retinal sections following ONC at different time points after ONC (6 hpi, 1, 2, 4, and 7 dpi). As published by Diekmann et al. [22], almost no AcT^+ RGCs or displaced amacrine cells in the RGCL were labeled with pS6 in naive retinas (Fig. 5a). However, 6 h after injury, there is a trend that ~6% of the RGCs (AcT^+, $CHAT^-$) were labeled with pS6 and this percentage increased until 24% at 1 day post-ONC. mTOR activation finally peaked 2 days after ONC and reached minimum levels again at 4 dpi (Fig. 5, $n = 3$, one-way ANOVA, $F_{(5,\ 12)} = 198{,}231$, $p < 0.0001$, Dunnet post-hoc test, p (Naive vs. 1 dpi) < 0.0001, p (naive vs. 2 dpi) < 0.0001).

To evaluate efficient mTOR inhibition after intravitreal administration of rapamycin (Rap), the same triple staining was performed on retinal sections following vehicle or rapamycin treatment at different time points after ONC (6 hpi, 1, 2, 4, and 7 dpi). In Fig. 5b, a clear increase in $pS6^+$ RGCs was observed in retinas of injured vehicle-treated fish, similar as after ONC without intravitreal injections, ruling out compromising effects of vehicle treatment on mTOR activation. Importantly, mTORC1 activation was clearly absent in rapamycin-treated fish at every time point (2 dpi is shown in Fig. 5b), thus

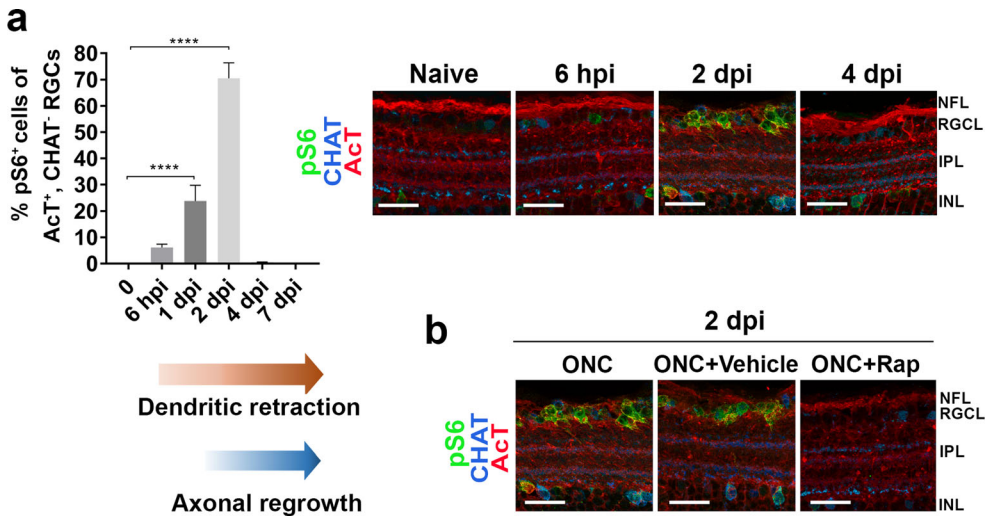

Fig. 5 Early retinal mTOR activation after ONC in adult zebrafish can be prevented using rapamycin injections. **a** Quantification of the mTOR activation pattern after ONC, using triple immunostainings for pS6 (mTOR activation), acetylated-tubulin (AcT), and choline acetyltransferase (CHAT), reveals an immediate 6% increase in the number of $pS6^+$, AcT^+, $CHAT^-$ RGCs, 6 h after ONC. At 2 days post-ONC, mTOR activation peaked, and then has decreased again 2 days later as at 4 dpi none or very few $pS6^+$ RGCs can be detected. Data represent mean ± SEM. **b** In contrast to uninjected or vehicle-injected eyes, no increase in mTOR activation is visible after intravitreal injection of rapamycin at 0 and 1 dpi, here shown at 2 dpi. Scale bar = 20 μm. *NFL* nerve fiber layer, *RGCL* retinal ganglion cell layer, *IPL* inner plexiform layer, *INL* inner nuclear layer, *Rap* rapamycin

indicating that an effective and sustained mTORC1 inhibition can be obtained in adult RGCs after intravitreal rapamycin injection (Fig. 5b).

Consistent with our previous observations, analysis of IPL thickness, Sv2, Znp-1, and Map2 retinal expression in naive and vehicle-treated fish at 4 dpi revealed a clear retinal synaptic decay and dendritic shrinkage after ONC (Fig. 6a–c). However, and most notably, IPL thickness, as well as Sv2, Znp-1, and Map2 expression values in retinal samples of rapamycin-treated fish at 4 dpi, still resembled baseline values, implying that fish with a reduced retinal mTOR activity were unable to retract their dendrites and degrade their synapses immediately after ONC (Fig. 6a–c, IPL measurements: $n = 9–10$, one-way ANOVA, $F_{(2,\ 25)} = 8.265$, $p = 0.002$, Dunnet post-hoc test, p (Naive vs. Vehicle) = 0.001. Sv2: $n = 9–13$, Kruskal-Wallis, Df = 2, $H = 7.157$, $p = 0.028$, Dunnet post-hoc test, p (Naive vs. Vehicle) = 0.02. Map2: $n = 12–14$, one-way ANOVA, $F_{(2,\ 36)} = 5.324$, $p = 0.009$, Dunnet post-hoc test, p (Naive vs. Vehicle) = 0.007). Of note, to ascertain immediate preservation of synapto-dendritic trees after mTOR inhibition, a Znp-1 staining was concurrently performed on retinal sections of vehicle- and rapamycin-treated fish at 1 dpi. In line with expectations, rapamycin-treated fish did not show a reduction in Znp-1 intensity as compared to naive fish, whereas clear synaptic degradation could already be observed in vehicle-treated retinas at 1 dpi (Fig. 6c).

To evaluate whether inhibition of retinal mTOR activation after ONC also interferes with RGC axonal regeneration, axons of naive and of vehicle- and rapamycin-treated fish were anterogradely traced with biocytin at 7 dpi and axonal regeneration was quantified at the level of the contralateral optic tectum as previously described [21]. Tectal innervation in naive fish was set as a 100% reference value. A 50% decrease in tectal reinnervation was observed in crushed fish injected with rapamycin as compared to injured vehicle-treated fish, which showed the expected reinnervation percentage of ~75% (Fig. 7). Misnavigation of regrowing RGC axons in the ipsilateral optic tectum was not observed (Fig. 7). Furthermore, rapamycin treatment did not affect cell survival, as activated caspase-3 stainings on retinal sections of naive, vehicle- and rapamycin-treated fish at 4 dpi did not unveil caspase-3 immunopositive cells (data not shown). These data then also confirm recently published observations that mTOR drives zebrafish optic nerve regeneration [22]. Interestingly, our data now suggest that inhibition of retinal mTOR activation after ONC immediately prevents retinal dendritic and synaptic deterioration after ONC, which later on results in a reduced RGC axonal regrowth capacity.

To further support this theory, optic tectum reinnervation was quantified after delayed rapamycin treatment (intravitreal injections at 4 and 5 dpi), when dendritic shrinkage has already occurred (Fig. 7, $n = 4–9$, one-way ANOVA, $F_{(4,\ 30)} = 49.805$, $p < 0.0001$, Tukey post-hoc test, p (Naive vs. Vehicle, Rap, Delayed Rap) < 0.0001, p (Naive vs. delayed vehicle) = 0.0012, p (Naive vs. Delayed Vehicle) = 0.0012, p (Vehicle vs. Rap) < 0.0001, p (Rap vs. Delayed Vehicle) < 0.0001, p (Rap vs. Delayed Rap) = 0.0003). As expected and already reported by Diekmann et al. [22], this delayed treatment did not negatively affect axonal regeneration, as there was no difference in optic tectum reinnervation after delayed

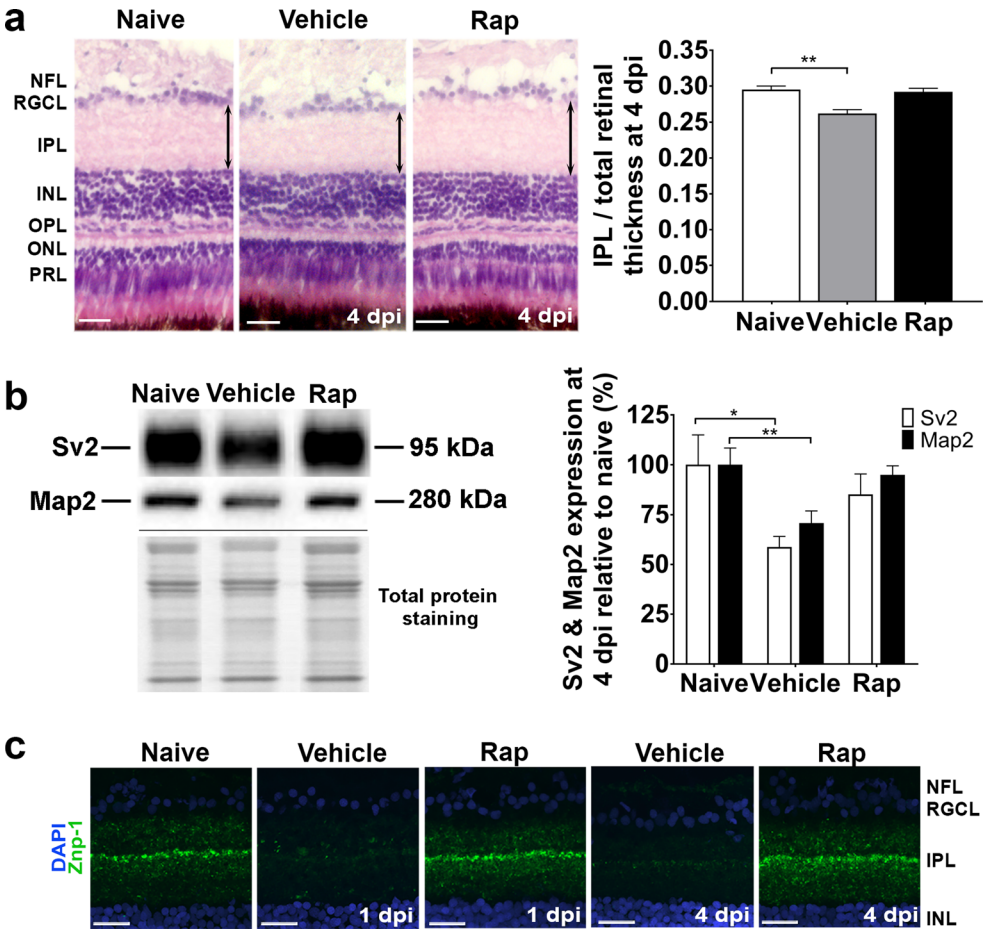

Fig. 6 Retinal mTOR inhibition prevents early retinal synaptic and dendritic degeneration after ONC. **a** Representative images of H&E-stained retinal sections and quantitative analysis of IPL/total retinal thickness reveal IPL thinning in vehicle-treated fish at 4 dpi as compared to naive fish, yet not in fish intravitreally injected with rapamycin at 0 and 1 dpi. Scale bar = 20 μm. Data represent mean ± SEM. **b** Representative picture and bar graph showing WB analysis data for Sv2 and Map2 on retinal extracts of naive and vehicle- or rapamycin-treated fish at 4 dpi, plotted as a relative percentage to naive fish. Significantly decreased Sv2 and Map2 protein levels were observed after vehicle treatment, respectively indicating synaptic and dendritic degeneration during RGC axonal regrowth. Rapamycin-treated fish did not show a decrease in Sv2, nor in Map2 protein, thus stating mTOR as a regulator of retinal synaptic and dendritic deterioration during RGC axonal regrowth. Swift membrane total protein staining served as loading control. Data represent mean ± SEM. **c** Immunostainings for Znp-1 on retinal sections of naive and vehicle- or rapamycin-treated fish at 1 or 4 dpi reveal a decrease in Znp-1 intensity in vehicle-treated but not in rapamycin-treated animals, again confirming mTOR as a driver of synaptic degeneration after ONC. DAPI (blue) was used as nuclear counterstain. Scale bar = 20 μm. *NFL* nerve fiber layer, *RGCL* retinal ganglion cell layer, *IPL* inner plexiform layer, *INL* inner nuclear layer, *OPL* outer plexiform layer, *ONL* outer nuclear layer, *PRL* photoreceptor layer, *Rap* rapamycin

rapamycin, immediate or delayed vehicle treatment. Together, these data indicate that the detrimental effect of early mTOR inhibition on axonal regeneration is, at least partly, caused by the lack of dendritic shrinkage and synaptic pruning.

Retinal Broad-Spectrum MMP Inhibition Consecutively Blocks Retinal Synaptic/Dendritic Degeneration and Disturbs RGC Axonal Regrowth After Optic Nerve Injury

We previously published that fish subjected to retinal broad-spectrum MMP inhibition, obtained via repeated intravitreal injections of GM6001, suffered from aberrant tectal reinnervation at 1 week after optic nerve injury [21]. Additional analyses in the retina now demonstrated that GM6001-treated fish do not show IPL thinning after ONC (Fig. 8a, $n = 6–8$, $F_{(2,\ 15)} = 7.415$, $p = 0.006$, Dunnet post-hoc test, p (Naive vs. Vehicle) = 0.005) and fail to significantly degrade retinal synapses and to retract their dendrites at least until 4 dpi as opposed to vehicle-treated fish, as shown by analysis of Sv2 and Map2 protein expression, respectively (Fig. 8b, Sv2: $n = 11–16$, Kruskal-Wallis, Df = 2, $H = 6.921$, $p = 0.033$, Dunnet post-hoc test, p (Naive vs. Vehicle) = 0.020. Map2: $n = 11–22$, Kruskal-Wallis, Df = 2, $H = 7.925$, $p = 0.031$, Dunnet post-hoc test, p (Naive vs. Vehicle) = 0.0363). This finding is in accordance with recent reports that support a critical role of dendrite–extracellular matrix (ECM) interactions—and thus of MMPs, which are well known for their

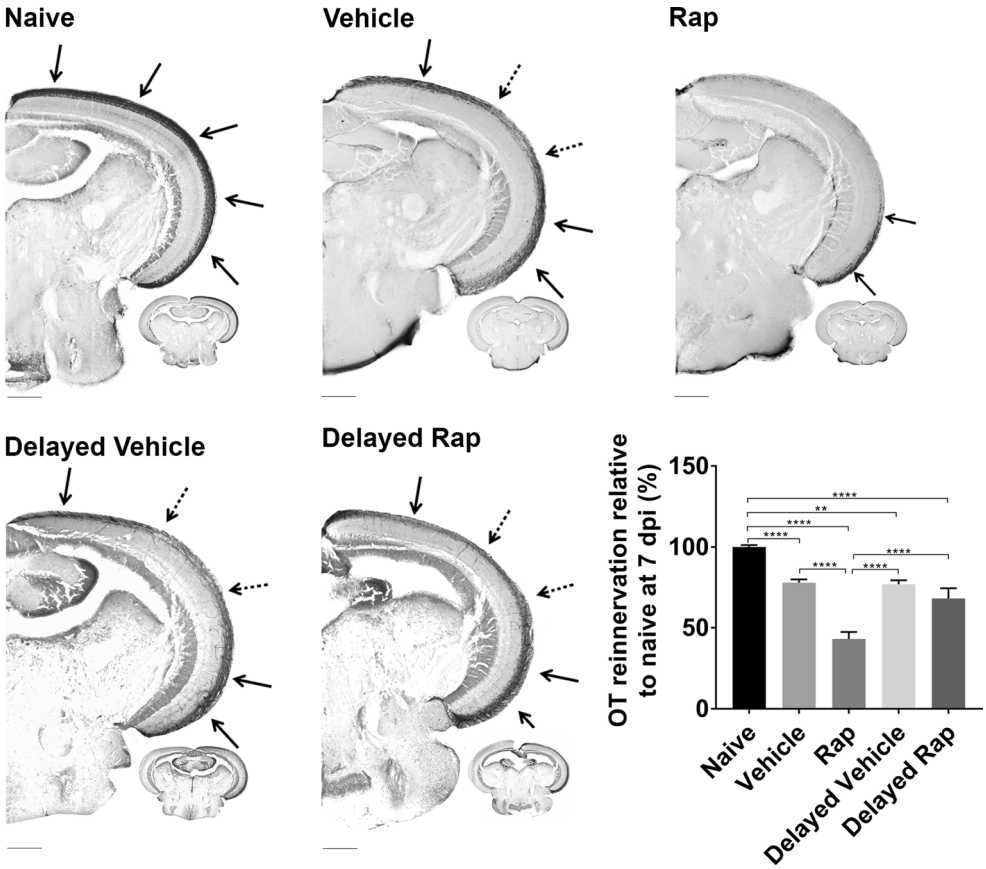

Fig. 7 Early retinal mTOR inhibition disturbs optic tectum reinnervation by regenerating RGC axons in adult zebrafish. Representative images and semi-quantitative analysis of the area covered by RGC axons in the optic tectum of naive and crushed vehicle- or rapamycin-treated fish reveal a clearly diminished reinnervated tectal area after intravitreal injections of rapamycin at 0 and 1 dpi as opposed to vehicle-treated and naive fish (indicated with black arrows). Notably, delayed mTOR inhibition, using rapamycin treatment at 4 and 5 dpi, did not affect axonal regeneration and tectal innervation as compared to vehicle-injected fish. Scale bar = 200 μm. Data represent mean ± SEM. *Rap* rapamycin, *OT* optic tectum

extensive ECM remodeling capacity—in maintaining neuronal dendrites and reactivating their structural plasticity in matured neuronal circuits [47, 48]. As such, and similar to the mTOR data, also GM6001-treated fish, known to have a decreased RGC axonal regrowth capacity upon ONC, primarily seem to suffer from an inability to degrade their synapto-dendritic compartments.

Discussion

While a distinct time frame for RGC axon growth versus dendrite expansion has been described during development of the retinofugal system, the temporal relationship between axon and dendrite regeneration in injured adult neurons remains largely unknown. Intriguingly, by using the zebrafish ONC model as an injury paradigm, we now demonstrate that mature regeneration-competent neurons are programmed to repeat the developmental order of neurite outgrowth upon injury, thus prioritizing axonal regeneration followed by dendritic regrowth [9, 17]. Notably, contradictory allegations have been made about the involvement of axon-target contact as the trigger for dendritogenesis during development. While some studies report that dendrites emerge from the cell body before the axon tip reaches its neuronal target, most emphasize the necessity of functional axon-target synapses to induce dendritic growth [9, 49–52]. Our work on adult regenerating RGCs supports the hypothesis that the establishment of novel synaptic contacts between primary arriving RGC axons and their neuronal targets in the brain could be an important trigger for initiating dendritic regrowth. Indeed, our data reveal that restoration of Znp-1 intensity in the brain at 10 days post-ONC coincides with a rise in retinal Map2 expression, thus pointing to a simultaneous generation of novel RGC pre-synaptic termini and retinal dendrites.

Importantly, and in contrast to developing neurons, adult neurons already possess an elaborate dendritic tree when faced with axotomy and the subsequent task to regrow their axons. Our data now reveal that adult CNS regenerating neurons undergo major dendritic retraction before they start to regrow their axons, and that they only begin to reconstruct their dendrites upon axonal target contact. These findings impose the question whether dendrites need to retract in order to boost RGC axonal regrowth. To address this "antagonistic axon-dendrite interplay" hypothesis, mTOR was chosen as a lead molecule as several publications reported mTOR as a major driver of vertebrate RGC axonal regeneration, but also denoted its importance in regulating RGC dendritic morphology upon axotomy in mammals [19, 24]. mTOR activity, which is highly involved in driving neuronal development, is reduced to low levels in adult mammalian neurons, and is reported to even further decrease upon axonal injury. Maintaining active

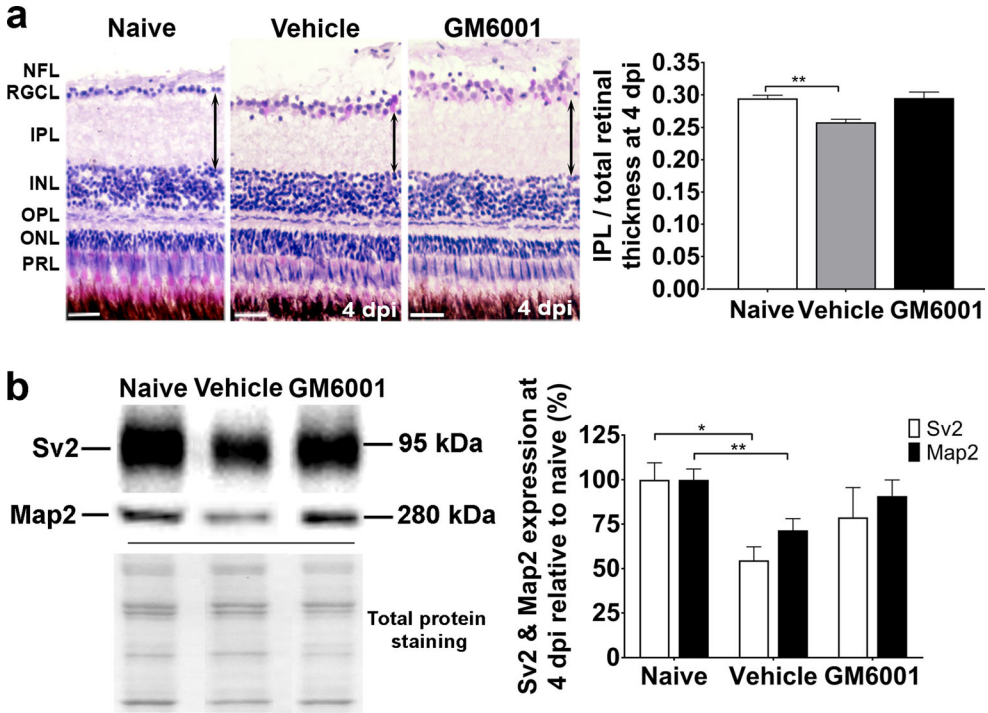

Fig. 8 Fish subjected to retinal broad-spectrum MMP inhibition, antecedently reported to show aberrant RGC axonal regrowth, suffer from an inability to degenerate retinal synapses and dendrites after ONC. **a** Representative images of H&E-stained retinal sections and quantitative analysis of IPL/total retinal thickness shows that, as opposed to vehicle-treated fish, IPL thinning does not occur at 4 dpi in fish intravitreally injected with GM6001 at 0 and 2 dpi. Data represent mean ± SEM. Scale bar = 20 μm. **b** Representative picture and bar graph showing WB analysis data for Sv2 and Map2 on retinal extracts of naive and vehicle- or GM6001-treated fish at 4dpi, plotted as a relative percentage to naive fish. In contrast to vehicle-treated fish, Sv2 and Map2 protein levels did not decrease in GM6001-treated fish, thus stating MMPs as regulators of retinal synaptic and dendritic deterioration after ONC. Swift membrane total protein staining served as loading control. Data represent mean ± SEM. *NFL* nerve fiber layer, *RGCL* retinal ganglion cell layer, *IPL* inner plexiform layer, *INL* inner nuclear layer, *OPL* outer plexiform layer, *ONL* outer nuclear layer, *PRL* photoreceptor layer

mTOR levels at a pre-injury status via phosphatase and tensin homolog (PTEN) deletion upon axonal lesion markedly increased the regenerative ability of injured adult RGCs in vivo, and thus promoted axonal regeneration [53]. Notably, while consistent upregulation of mTOR activity is needed to drive axonal regeneration in mammals, Diekmann et al. [22] only observed a short and immediate peak in mTOR activity after ONC in adult zebrafish RGCs. Interference with this early burst in mTOR activation via systemic rapamycin treatment partially reduced RGC axonal regrowth from 2.5 dpi onwards, and compromised functional recovery [22]. Yet, potential effects on dendrite retraction upon rapamycin treatment remained unmonitored. In order to explore if mTOR inhibition could affect early dendrite shrinkage after injury, we first showed that mTOR is active in a subset of fish RGCs from 6 hpi on. Next, we confirmed that local inhibition of mTOR activation, immediately after ONC, indeed reduces RGC axonal regeneration, but importantly, also completely prevents dendritic retraction/synaptic decay. Moreover, as dendrites already retract before axons start to regrow (cfr. no visible Gap-43 induction in intraretinal RGC axons until 2 dpi [39], and no significant *gap-43* mRNA induction at 1 dpi, but already a significant decrease in Map2 protein levels at this time point in our study, Fig. 3a and Fig. 2), it is plausible to speculate that the incapacity of regeneration-competent neurons to decently regrow RGC axons upon mTOR inhibition might follow directly from their inability to first retract their dendrites.

Surprisingly, this observation, that mTOR activity is likely needed for dendrites to retract in adult zebrafish, is in contrast with published data in mammals. A study by Morquette et al. (2015) showed that early RGC dendrite degeneration upon axotomy in mice can be prevented by RNA-mediated knockdown of regulated in development and DNA damage response 2 (REDD2), an inhibitor of mTOR [3]. Nonetheless, mTOR driving dendritic retraction in injured adult zebrafish can be linked to leukemia inhibitory factor (LIF) functioning in this model. Indeed, in adult zebrafish, the expression of LIF, which is reported to activate the PI3K/AKT/mTOR pathway in rodents [54], strongly coincides with the mTOR activity burst after ONC [22, 55]. Moreover, LIF has been reported to cause major dendrite retraction of rat sympathetic neurons in vitro [56], and is observed to drive optic nerve regeneration in zebrafish [55]. Overall, we can conclude that the intrinsic mTOR activity pattern in both naive and injured RGCs fundamentally differs between zebrafish and mammals, as well as the pathways via which mTOR is driven to affect dendritic

remodeling. These important differences in mTOR regulation could therefore well underlie the distinct regenerative capacities between mammals and fish, and encourages further in-depth investigation.

Strikingly, this apparent antagonistic interplay between dendrites and axons in injured mature neurons is reinforced by the fact that fish exposed to retinal MMP inhibition after ONC also showed a consecutive inability to degrade their dendrites and regrow their axons. MMPs have been previously reported as regulators of dendrite degradation upon neuronal injury, e.g., in larval *Drosophila melanogaster*, wherein severed dendrites of sensory neurons failed to degenerate in Mmp-1 and Mmp-2 mutants, while wild-type neurons showed consecutive dendritic clearance and regrowth after injury [25]. Moreover, our lab recently observed a clear upregulation of Mmp-9, -13 and -14a protein levels in IPL dendrites/synapses during distinct phases of retinotectal regeneration, likely implicating these proteinases in retinal dendritic and synaptic remodeling in adult zebrafish after ONC [21]. Of note, MMPs have also been described as drivers of CNS axonal (re)growth, mainly via degrading inhibitory molecules around the injury site, thereby clearing the path for axons to regrow [20, 57–59]. Yet, we administered GM6001 intravitreally and therefore likely inhibited MMP functioning primarily at the level of the retina and not in the optic nerve. Furthermore, the CNS injury site in adult zebrafish is increasingly acknowledged to show little scarring or expression of inhibitory molecules [5, 21]. As such, it seems implausible that retinal MMP inhibitor application exclusively caused a direct inhibitory effect on RGC axonal regrowth.

Overall, the consecutive perturbation of dendritic shrinkage/synaptic deterioration and RGC axonal regrowth after ONC, seen in rapamycin- and GM6001-treated fish, suggests that transient RGC dendritic shrinkage might be conditional for axonal regeneration upon optic nerve injury. Moreover, it unveiled the involvement of intrinsic (e.g., mTOR), as well as extrinsic (e.g., MMPs) signaling pathways in this dendrite-axon interplay. This study therefore emphasizes the importance of monitoring/manipulating RGC dendritic remodeling upon optic nerve injury in mammalian optic neuropathy models, as a potential means to obtain successful CNS regeneration.

Remarkably, the causal/antagonistic link between dendritic remodeling and axonal regeneration is not an established idea as only two papers hint toward this connection. Chung et al. (2016) reported that concurrent severing of the ASJ axon and sensory dendrites in larval and young *C. elangs* significantly enhanced axonal regrowth, as compared to ASJ neurons subjected to axotomy alone [60]. Also in mice, it has been observed that viral vector-mediated ciliary neurotrophic factor (CNTF) administration after acute axonal injury, which turns α-RGCs in a highly regenerative state, causes an increased reduction in RGC dendritic complexity as compared to axonal injury alone [61]. Altogether, these (reported and our current) findings reveal a conserved neuronal remodeling mechanism upon injury in both adult invertebrate and vertebrate nervous systems. Moreover, it has been described that developing mammalian neurons, e.g., RGCs, irreversibly switch from an axonal to a dendritic growth mode, which has been put forward as a reason for the inability of adult CNS neurons to regenerate in vivo [62]. As it is assumed that this "switch signal" represents a contact-mediated or membrane-associated signal from amacrine cells, substantial loss of synaptic contacts and subsequent dendritic shrinkage upon injury, as seen in adult zebrafish subjected to ONC, might pose an important means for adult neurons to regain their axonal regrowth mode [9, 62].

As this research is utterly novel, the underlying processes for mature dendrites restricting axonal regrowth in adult neurons remains open for speculation. In this respect, Chung et al. (2016) suggested that neuronal activity might form the regulatory mechanism controlling axonal regrowth, as inhibition of ASJ sensory input by means of dendrite cutting or through mutations in L-type calcium channels enhanced axonal regeneration. Furthermore, a novel regulatory mechanism that differentially directs axon and dendrite growth in larval *D. melanogaster* class IV dendritic arborization neurons, so-called bimodal controllers, has been discovered. In detail, highwire, an E3 ubiquitin ligase belonging to the dual leucine zipper kinase (DLK) signaling pathway, prevents axonal growth while driving dendritic growth within the same neuron in vivo by directing Fos and Knot, two downstream transcription factors that mediate axonal and dendritic regulation, respectively [18]. Alternatively, it is known that both developing and mature neurons are highly energy-demanding and that not only their basal function but also their growth potential heavily relies on adequate energy supply [17, 63, 64]. In line with this, AMP-activated protein kinase (AMPK) has been shown to function as an energy sensor during multiple stages of hippocampal neuronal development. Here, energy stress activates AMPK, leading to either suppression of axogenesis or secondary dendritic growth, depending on early or late stressor induction [17].

All this information combined then also inspired us to postulate that axonal and dendritic growth in the vertebrate CNS occur consecutively rather than simultaneously—both during development and regeneration—due to cellular metabolic restriction. Notably, adult neurons need high energy levels (up to 60% of mitochondrially provided ATP) to maintain their dendrites/synapses and also axonal regrowth requires massive ATP consumption for the formation of an active growth cone [65–67]. Moreover, it is known that a reduction in neuronal activity can relieve dendritic mitochondria from their role in maintaining synapses and increase dendritic mitochondrial mobility [63]. We therefore hypothesize that dendritic retraction might occur before axonal regeneration to provide the necessary energy/nutrient funneling toward the axonal growth cone and simultaneously reassure cellular homeostasis.

Notably, a recent study showed that enhancing mitochondrial transport toward axons after sciatic nerve crush in mice, via deletion of mitochondria-anchoring protein syntaphilin (SNPH), accelerates axonal regeneration, thus reinforcing that restoring adequate mitochondrial trafficking and ATP supply after neuronal injury are indeed central to axonal regrowth [68]. This statement has recently been invigorated in an in vitro study, in which mouse cortical neurons after co-deletion of PTEN and suppressor of cytokine signaling 3 (SOCS3), a paradigm known to promote axonal regrowth, showed increased mitochondrial transport as compared to control neurons [69].

Of note, we deliberately opted to longitudinally characterize the axon-dendrite interplay after ONC via spatiotemporal analysis of dendritic, synaptic, and axonal markers. This because in vivo time-lapse recording of this interaction at single cell level in an adult zebrafish, would require assessment of RGC dendritic responses in the IPL and axonal regrowth in the optic nerve at the same time, which is, to date, not attainable. Furthermore, while we provide good first indications that dendritic remodeling upon ONC in regeneration-competent neurons might serve as fuel for axonal regeneration, causal evidence for this axon-dendrite antagonistic interplay is still lacking. A future in vivo proof-of-concept would likely imply interfering with growth-/energy-regulating molecules in a cellular compartment-specific way, as most molecules involved in axonal morphogenesis equally regulate dendritic morphogenesis and vice versa [70]. As, to our knowledge, successful neuronal compartment-specific gene/protein manipulation remains undocumented, this predicts to be a challenging task to fulfill. Instead, interfering with dendritic retraction of injured adult regeneration-competent neurons after axotomy in vitro and analyzing the effect on axonal regrowth might present a more achievable approach toward first conclusive results.

Overall, our data reinforce recent observations made on invertebrate neurons and indicate the existence of a novel regulatory mechanism that orchestrates dendrite-axon interactions in mature regeneration-competent vertebrate CNS neurons. Unraveling the genetics of the signaling pathways underlying remodeling of the dendritic compartment after optic nerve injury might then also form an intriguing strategy and a refreshing view on promoting axonal regrowth in the injured mammalian CNS.

Materials and Methods

Zebrafish Maintenance

Zebrafish (*Danio rerio*) were maintained under standard laboratory conditions at 28 °C on a 14 h light/10 h dark cycle. Fish were fed twice daily with a combination of dry food and brine shrimp. All experiments were performed on equally sized, 5-month-old adult zebrafish of either sex (AB wild-type) and were approved by the KU Leuven Animal Ethics Committee and executed in strict accordance with the European Communities Council Directive of 20 October 2010 (2010/63/EU).

Optic Nerve Crush

Optic nerve crush (ONC) on adult zebrafish was performed as previously described [21]. Briefly, zebrafish were anesthetized in a buffered 0.03% solution of tricaine (MS-222, Sigma-Aldrich) and put under a dissecting microscope (Leica) on moist tissue paper, left side facing upward. After removal of the surrounding connective tissue, the eyeball was lifted out of its orbit, thereby exposing the optic nerve and ophthalmic artery. Sterile forceps were carefully placed around the left optic nerve, which was crushed for 10 s at 0.5 mm distance of the optic nerve head, thereby avoiding damage to the ophthalmic artery. A successful ONC was indicated by the appearance of a clear gap inside the translucent nerve sheath. Fish were returned to system water in separate tanks to recover.

Real-Time Polymerase Chain Reaction

Quantitative real-time polymerase chain reaction (RT-qPCR) was used to measure the transcript levels of *gap-43* before and at early time points after ONC injury (6 hpi, 1 dpi, 4 dpi). Thereto, fish were euthanized using 0.1% tricaine, after which retinas were quickly dissected on ice and pooled per three. The tissues were digested using Tri Reagent (Sigma-Aldrich) before total RNA isolation using the NucleoSpin RNA isolation kit (Machery-Nagel). Oligo dT primers and Superscript III reverse transcriptase (Invitrogen, Belgium) were used to execute reverse transcription reactions to synthesize cDNA, followed by RT-qPCR using SYBR Green Mastermix (Bio-Rad), 250 nM of both primers, and a CFX96 Real-Time detection system (Bio-Rad). Both the *gap-43* FW (5′-CAGC CGACGTGCCTGAA-3′) and *gap-43* REV (5′-TCCT CAGCAGCGTCTGGTTT-3′) primers were already used to detect *gap-43* mRNA levels in zebrafish [40]. Samples were run in duplicate with 56 °C as annealing temperature. Gene expression was finally analyzed using GeNorm (qBase software, [71]) and normalized against two housekeeping genes (hypoxanthine phosphoribosyl-transferase 1 (*hprt1*) and succinate dehydrogenase complex subunit A flavoprotein (*sdha*)).

Histology, Immunohistochemistry, and Histomorphometric Analysis

For all immunohistochemical (IHC) stainings, fish were euthanized by submersion in buffered 0.1% tricaine. After transcardial perfusion with phosphate-buffered saline (PBS,

0.01 M, pH 7.4) and 4% paraformaldehyde (PFA) in PBS, eyes/brains of adult fish were dissected at various stages post-injury (at baseline (naive) and at 6 hpi, 1, 4, 7, 10, 14, and 18 dpi). Hereafter, the tissues were post-fixed overnight in 4% PFA in PBS and kept in 30% sucrose in PBS until further processing for cryosectioning. Ten-micrometer-thick sagittal sections of the retina and 10-μm transverse brain sections, taken at the level of the optic tecti, were made. Of note, retinal Psd-95 immunostaining was conducted on retinal cryosections briefly fixated with 4% PFA for 30′ upon dissection. Immunostainings for Psd-95, Znp-1, phosphorylated S6 (pS6), acetylated-tubulin (AcT), choline acetyltransferase (CHAT), and Map2 were performed using the following primary antibodies: mouse anti-Psd-95 (1:500, Abcam, ab2723), mouse anti-Znp-1 (1:1000, Developmental Studies Hybridoma Bank), rabbit anti-pS6 (1:200, Cell Signaling Technology), mouse anti-acetylated-tubulin (1:1000, Sigma), goat anti-choline acetyl transferase (1:100, Millipore), mouse anti-Map2 (1:2000, Sigma, M1406) and were detected with Alexa conjugated secondary antibodies or horseradish peroxidase (HRP)-labeled antibodies (Dako), using the TSA™ FT/Cy3 System (PerkinElmer). Retinal/brain sections from at least three fish per post-injury stage were stained. All immunolabelings were visualized with an Olympus FV1000 confocal microscope at × 60 magnification. Retinal morphology was studied at baseline, 6hpi, 1, 4, 7, 10, and 14 dpi by H&E staining on retinal sections. Histological pictures were acquired with a microscope Zeiss imager Z1 at × 20 magnification. For morphometric analysis of the ratio IPL/total retinal thickness, the IPL and total retinal thickness were measured in the central retina on both sides adjacent to the optic nerve on six mid-sagittal retinal sections (80 μm apart) per fish, using ImageJ software. For characterization of mTOR activation, a triple labeling was performed for pS6, AcT, and CHAT, and the percentage of cells positive for pS6 was quantified in relation to the AcT positive cells in the RGCL on at least four sections of three different fish. Cells that were immunopositive for CHAT in the RGCL were excluded as they represent displaced amacrine cells.

Western Blotting

After fish were sacrificed in buffered 0.1% tricaine, retinas were dissected at baseline (naive), 6 hpi, 1, 4, 7, 10, 14, or 18 dpi after ONC and homogenized in lysis buffer (10 mM Tris-HCl pH 8, 1% Triton X-100, 150 mM NaCl, 0.1% SDS, 0.5% sodium deoxycholate, 0.2% sodium azide), supplemented with protease inhibitors (Roche). Homogenates were loaded at 10 μg onto 4–12% Bis-Tris gels (Bio-Rad) and transferred onto a nitrocellulose membrane (Bio-Rad). Overnight incubation with mouse anti-SV2 (1:1000, Developmental Studies Hybridoma Bank) or mouse anti-Map2 (1:1000, Sigma-Aldrich, M9942) primary antibodies was followed by 45′ incubation with goat anti-mouse HRP-conjugated antibody (Dako). Protein bands were visualized using a luminol-based enhanced chemiluminescent kit (Thermo Scientific) by means of an imaging system (Bio-Rad, ChemiDoc MP imaging system), and semi-quantitatively evaluated by densitometry (Image Lab 4.1, Bio-Rad). Swift membrane total protein staining (G-Biosciences) of the nitrocellulose membrane served as loading control and was used for normalization of protein values. Data were plotted as a relative percentage to and statistically compared to the baseline (naive) condition, which was set as 100%. For longitudinal studies (cfr. Fig. 2), data were collected from at least three retina samples per time point. For rapamycin (Rap) and GM6001 treatment experiments, at least nine retina samples were used per condition.

Dorsal Light Reflex

The dorsal light reflex (DLR) was used to assess functional recovery of primary vision after an optic nerve lesion in adult zebrafish [44, 45]. A total of nine adult zebrafish was subjected to a DLR at 10, 12, 14, and 18 dpi. In brief, fish were put in a cylindrical container, filled with system water, of 500 mm long and 120 mm in diameter. First, a light source was slowly rotated from the dorsal (0°) to the right lateral side of the fish (90°), ultimately giving sole input to the right eye. Since the right optic nerve was uninjured, fish were expected to show a normal inclination of their dorsoventral axis in this setup, thus serving as an internal control. Next, the left crushed eye of the fish was subjected to the same protocol. The response of the adult fish was divided into three categories, based on the position of the light-exposed eye relative to the non-light-exposed eye at the end of the DLR, when the light source was positioned completely lateral (90°): a "full DLR" corresponds to a fish where the body axis completely followed the movement of the light bundle, resulting in a position of the light-exposed eye below the non-light-exposed eye, when drawing a fictive horizontal line through both eyes. During a "partial DLR," the fish did show body axis tilting but maximally tilted in such a way that the targeted eye was not completely located beneath the non-targeted eye. Fish with "no DLR" did not respond to the moving light influx at all and thus did not tilt their body axis, which indicated a pronounced default in basic visual perception.

Retinal mTORC1 and Broad-Spectrum Matrix Metalloproteinase Inhibition

The effect of retinal mTORC1 inhibition on zebrafish retinotectal regeneration was studied using intravitreal injections with 300 nl of 20 μM Rapamycin (LC Laboratories) at 0 and 1 dpi using a micro-injector (UMP3, World Precision Instruments). To study if delayed rapamycin treatment would still interfere with axonal regeneration, rapamycin and the

vehicle were also injected at 4 and 5 dpi. Alternatively, to obtain retinal broad-spectrum matrix metalloproteinase (MMP) inhibition, 300 nl of 5 mM GM6001 (Santa Cruz, sc-203979) was IVT injected at 0 and 2 dpi. Both naive and vehicle- (rapamycin: 5% DMSO in PBS; GM6001: 10% DMSO in PBS) injected fish were implemented in the experimental set-ups as controls.

Tracing and Quantification of Tectal (Re)Innervation

Regenerating axons from the retina toward the optic tectum were visualized by means of biocytin tracing and tectal reinnervation was analyzed as previously described [21, 41]. In short, biocytin, taken up by the regenerated axons, was visualized on 50-μm coronal vibratome sections by means of a Vectastain ABC kit (Vector laboratories), using diaminobenzidine as chromogen. Sections were dried on gelatin-coated slides and counterstained with neutral red solution to allow for brain nuclei identification. Brain sections through the central optic tecti were identified based on the presence of specific nuclei [72] and histological photographs were acquired with a microscope Zeiss imager Z1 at × 10 magnification. Tectal (re)innervation was quantified via an in house developed ImageJ script, in which the biocytin-labeled area was measured using a preset threshold. Next, axonal density was defined as the ratio of the biocytin$^+$ area to the area of reinnervation, being the SFGS and SO of the optic tectum. Per fish, tectal reinnervation was analyzed on at least five sections containing the central optic tectum, using 4–9 fish per condition. Of note, in all experiments, naive fish were included, in which tectal innervation was analyzed and set as a 100% reference value. Reinnervation values obtained from the injury conditions were expressed in percent relative to this reference control.

In addition, tectal reinnervation was investigated in Tg(*fGap-43*:*GFP*) zebrafish, which express green fluorescent protein (GFP) under the control of a GAP-43 promotor [39]. Images of at least four transverse brain sections of three different fish per time point were obtained using an Olympus FV1000 confocal microscope at × 20 magnification and analysis was performed using the methodology described above. As Gap-43 is not expressed in non-injured fish, the Gap-43 immunopositive tectal area of fish at 14 dpi was used as a reference and set as 100%, as this was the time point of complete innervation and maximum value.

Statistical Analysis

The image processing software ImageJ was used for all IPL thickness and optic tectum reinnervation analyses. To reduce bias and orientation-determined variability in morphometric IPL thickness and optic tectum reinnervation analysis, only sections through the central retina and central optic tectum were used. Furthermore, these analyses were always conducted on at least four sections per animal (technical replicates). To reduce the risk for bias during WB analysis, protein bands were automatically detected and evaluated by Image Lab 4.1 software (Bio-Rad). Furthermore, total protein staining was used for normalization of protein values. To analyze spatial/temporal differences in protein signal intensity on retinal sections in an unbiased way, intensities were always compared on at least three sections per animal (technical replicates) and were analyzed independently and blinded for the condition by two researchers. Also DRL was performed simultaneously by two researchers and scored after consensus.

All data are represented as mean ± SEM, except the RT-qPCR data for *gap-43* in which mean fold change values, relative to naive ± SEM are shown. The value of n represents the number of animals used per condition (biological replicates). All statistical tests were performed using Graphpad Prism 7.03. In all cases, raw data were tested for normal distribution using the Kolmogorov-Smirnov normality test and variance between groups was checked via the Brown-Forsythe's test for equality of variances. To evaluate a difference in optic tectum reinnervation at 0 and 10 dpi, a two-tailed Student's t test was performed. To compare three or more independent groups, a one-way ANOVA was performed if the data showed a normal distribution and variances between groups were homogeneous. A Dunnet or Tukey post-hoc test was performed and only the p values indicating a significant difference between two values/conditions are shown. When the ANOVA assumptions were violated, a Kruskal-Wallis test was used. DLR data were analyzed using Chi-square statistics. $P < 0.05$ was considered statistically significant.

Acknowledgements The authors thank Lut Noterdaeme and Marijke Christiaens for their technical assistance. This work was supported by the FWO (Fonds voor Wetenschappelijk Onderzoek) Flanders-Quebec bilateral research grant and by national grants from the Research Council of KU Leuven (KU Leuven BOF-OT/14/064), the Research Foundation Flanders (FWO G0B2315N) and Hercules Foundation (equipment grants AKUL/09/038 & AKUL/13/09). KL is a postdoctoral fellow funded by KU Leuven and AB is supported by L'Oréal-UNESCO "For women in science" (FWO-Vlaanderen, Belgium). IB holds an FWO PhD fellowship and JVH and EL is supported by the Flemish government agency for Innovation by Science and Technology (IWT-Vlaanderen, Belgium). LA is supported by KU Leuven. We want to thank Dr. Udvadia (University of Wisconsin) for providing Tg(*fGap-43*:*GFP*) zebrafish.

Compliance with Ethical Standards

Conflict of Interest The authors declare that they have no conflict of interest.

Ethical Approval Animal experiments were approved by the KU Leuven Animal Ethics Committee and executed in strict accordance with the European Communities Council Directive of 20 October 2010 (2010/63/EU).

References

1. Della Santina L, Inman DM, Lupien CB, Horner PJ, Wong RO (2013) Differential progression of structural and functional alterations in distinct retinal ganglion cell types in a mouse model of glaucoma. J Neurosci 33(44):17444–17457. https://doi.org/10.1523/JNEUROSCI.5461-12.2013
2. Pang JJ, Frankfort BJ, Gross RL, Wu SM (2015) Elevated intraocular pressure decreases response sensitivity of inner retinal neurons in experimental glaucoma mice. Proc Natl Acad Sci U S A 112(8):2593–2598. https://doi.org/10.1073/pnas.1419921112
3. Morquette B, Morquette P, Agostinone J, Feinstein E, McKinney RA, Kolta A, Di Polo A (2015) REDD2-mediated inhibition of mTOR promotes dendrite retraction induced by axonal injury. Cell Death Differ 22(4):612–625. https://doi.org/10.1038/cdd.2014.149
4. Benowitz LI, He Z, Goldberg JL (2015) Reaching the brain: advances in optic nerve regeneration. Exp Neurol 287:365–373. https://doi.org/10.1016/j.expneurol.2015.12.015
5. Becker T, Becker CG (2014) Axonal regeneration in zebrafish. Curr Opin Neurobiol 27:186–191. https://doi.org/10.1016/j.conb.2014.03.019
6. Drummond ES, Rodger J, Penrose M, Robertson D, Hu Y, Harvey AR (2014) Effects of intravitreal injection of a Rho-GTPase inhibitor (BA-210), or CNTF combined with an analogue of cAMP, on the dendritic morphology of regenerating retinal ganglion cells. Restor Neurol Neurosci 32(3):391–402. https://doi.org/10.3233/RNN-130360
7. Rodger J, Drummond ES, Hellstrom M, Robertson D, Harvey AR (2012) Long-term gene therapy causes transgene-specific changes in the morphology of regenerating retinal ganglion cells. PLoS One 7(2):e31061. https://doi.org/10.1371/journal.pone.0031061
8. Choi JH, Law MY, Chien CB, Link BA, Wong RO (2010) In vivo development of dendritic orientation in wild-type and mislocalized retinal ganglion cells. Neural Dev 5:29. https://doi.org/10.1186/1749-8104-5-29
9. Goldberg JL, Klassen MP, Hua Y, Barres BA (2002) Amacrine-signaled loss of intrinsic axon growth ability by retinal ganglion cells. Science 296(5574):1860–1864. https://doi.org/10.1126/science.1068428
10. Kizil C, Kaslin J, Kroehne V, Brand M (2012) Adult neurogenesis and brain regeneration in zebrafish. Dev Neurobiol 72(3):429–461. https://doi.org/10.1002/dneu.20918
11. Fimbel SM, Montgomery JE, Burket CT, Hyde DR (2007) Regeneration of inner retinal neurons after intravitreal injection of ouabain in zebrafish. J Neurosci 27(7):1712–1724. https://doi.org/10.1523/JNEUROSCI.5317-06.2007
12. Kroehne V, Freudenreich D, Hans S, Kaslin J, Brand M (2011) Regeneration of the adult zebrafish brain from neurogenic radial glia-type progenitors. Development 138(22):4831–4841. https://doi.org/10.1242/dev.072587
13. Wan J, Goldman D (2016) Retina regeneration in zebrafish. Curr Opin Genet Dev 40:41–47. https://doi.org/10.1016/j.gde.2016.05.009
14. Alunni A, Bally-Cuif L (2016) A comparative view of regenerative neurogenesis in vertebrates. Development 143(5):741–753. https://doi.org/10.1242/dev.122796
15. Bollaerts I, Veys L, Geeraerts E, Andries L, De Groef L, Buyens T, Salinas-Navarro M, Moons L et al (2017) Complementary research models and methods to study axonal regeneration in the vertebrate retinofugal system. Brain Struct Funct 223:545–567. https://doi.org/10.1007/s00429-017-1571-3
16. Gemberling M, Bailey TJ, Hyde DR, Poss KD (2013) The zebrafish as a model for complex tissue regeneration. Trends Genet 29(11):611–620. https://doi.org/10.1016/j.tig.2013.07.003
17. Ramamurthy S, Chang E, Cao Y, Zhu J, Ronnett GV (2014) AMPK activation regulates neuronal structure in developing hippocampal neurons. Neuroscience 259:13–24. https://doi.org/10.1016/j.neuroscience.2013.11.048
18. Wang X, Kim JH, Bazzi M, Robinson S, Collins CA, Ye B (2013) Bimodal control of dendritic and axonal growth by the dual leucine zipper kinase pathway. PLoS Biol 11(6):e1001572. https://doi.org/10.1371/journal.pbio.1001572
19. Berry M, Ahmed Z, Morgan-Warren P, Fulton D, Logan A (2016) Prospects for mTOR-mediated functional repair after central nervous system trauma. Neurobiol Dis 85:99–110. https://doi.org/10.1016/j.nbd.2015.10.002
20. Andries L, Van Hove I, Moons L, De Groef L (2017) Matrix metalloproteinases during axonal regeneration, a multifactorial role from start to finish. Mol Neurobiol 54(3):2114–2125. https://doi.org/10.1007/s12035-016-9801-x
21. Lemmens K, Bollaerts I, Bhumika S, de Groef L, Van Houcke J, Darras VM, Van Hove I, Moons L (2016) Matrix metalloproteinases as promising regulators of axonal regrowth in the injured adult zebrafish retinotectal system. J Comp Neurol 524(7):1472–1493. https://doi.org/10.1002/cne.23920
22. Diekmann H, Kalbhen P, Fischer D (2015) Active mechanistic target of rapamycin plays an ancillary rather than essential role in zebrafish CNS axon regeneration. Front Cell Neurosci 9:251. https://doi.org/10.3389/fncel.2015.00251
23. Jaworski J, Sheng M (2006) The growing role of mTOR in neuronal development and plasticity. Mol Neurobiol 34(3):205–219. https://doi.org/10.1385/MN:34:3:205
24. Di Polo A (2015) Dendrite pathology and neurodegeneration: focus on mTOR. Neural Regen Res 10(4):559–561. https://doi.org/10.4103/1673-5374.155421
25. Kuo CT, Jan LY, Jan YN (2005) Dendrite-specific remodeling of Drosophila sensory neurons requires matrix metalloproteases, ubiquitin-proteasome, and ecdysone signaling. Proc Natl Acad Sci U S A 102(42):15230–15235. https://doi.org/10.1073/pnas.0507393102
26. Szklarczyk A, Lapinska J, Rylski M, McKay RD, Kaczmarek L (2002) Matrix metalloproteinase-9 undergoes expression and activation during dendritic remodeling in adult hippocampus. J Neurosci 22(3):920–930
27. Lin YC, Koleske AJ (2010) Mechanisms of synapse and dendrite maintenance and their disruption in psychiatric and neurodegenerative disorders. Annu Rev Neurosci 33:349–378. https://doi.org/10.1146/annurev-neuro-060909-153204
28. Battista AG, Ricatti MJ, Pafundo DE, Gautier MA, Faillace MP (2009) Extracellular ADP regulates lesion-induced in vivo cell proliferation and death in the zebrafish retina. J Neurochem 111(2):600–613. https://doi.org/10.1111/j.1471-4159.2009.06352.x
29. Yazulla S, Studholme KM (2001) Neurochemical anatomy of the zebrafish retina as determined by immunocytochemistry. J Neurocytol 30(7):551–592
30. Meyer MP, Trimmer JS, Gilthorpe JD, Smith SJ (2005) Characterization of zebrafish PSD-95 gene family members. J Neurobiol 63(2):91–105. https://doi.org/10.1002/neu.20118
31. Liu Q, Londraville R, Marrs JA, Wilson AL, Mbimba T, Murakami T, Kubota F, Zheng W et al (2008) Cadherin-6 function in zebrafish retinal development. Developmental neurobiology 68(8):1107–1122. https://doi.org/10.1002/dneu.20646

32. Fox MA, Sanes JR (2007) Synaptotagmin I and II are present in distinct subsets of central synapses. J Comp Neurol 503(2):280–296. https://doi.org/10.1002/cne.21381
33. Riederer B, Matus A (1985) Differential expression of distinct microtubule-associated proteins during brain development. Proc Natl Acad Sci U S A 82(17):6006–6009
34. Matus A (1991) Microtubule-associated proteins and neuronal morphogenesis. J Cell Sci Suppl 15:61–67
35. Lieven CJ, Millet LE, Hoegger MJ, Levin LA (2007) Induction of axon and dendrite formation during early RGC-5 cell differentiation. Exp Eye Res 85(5):678–683. https://doi.org/10.1016/j.exer.2007.08.001
36. Okabe S, Shiomura Y, Hirokawa N (1989) Immunocytochemical localization of microtubule-associated proteins 1A and 2 in the rat retina. Brain Res 483(2):335–346
37. Faruki S, Doree M, Karsenti E (1992) cdc2 kinase-induced destabilization of MAP2-coated microtubules in Xenopus egg extracts. J Cell Sci 101(Pt 1):69–78
38. Cabrera JR, Lucas JJ (2016) MAP2 splicing is altered in Huntington's disease. Brain Pathol 27:181–189. https://doi.org/10.1111/bpa.12387
39. Diekmann H, Kalbhen P, Fischer D (2015) Characterization of optic nerve regeneration using transgenic zebrafish. Front Cell Neurosci 9:118. https://doi.org/10.3389/fncel.2015.00118
40. McCurley AT, Callard GV (2010) Time course analysis of gene expression patterns in zebrafish eye during optic nerve regeneration. J Exp Neurosci 2010(4):17–33
41. Bhumika S, Lemmens K, Vancamp P, Moons L, Darras VM (2015) Decreased thyroid hormone signaling accelerates the reinnervation of the optic tectum following optic nerve crush in adult zebrafish. Mol Cell Neurosci 68:92–102. https://doi.org/10.1016/j.mcn.2015.04.002
42. Udvadia AJ (2008) 3.6 kb genomic sequence from Takifugu capable of promoting axon growth-associated gene expression in developing and regenerating zebrafish neurons. Gene Expr Patterns 8(6):382–388. https://doi.org/10.1016/j.gep.2008.05.002
43. Nevin LM, Robles E, Baier H, Scott EK (2010) Focusing on optic tectum circuitry through the lens of genetics. BMC Biol 8:126. https://doi.org/10.1186/1741-7007-8-126
44. Brodsky MC (1999) Dissociated vertical divergence: a righting reflex gone wrong. Arch Ophthalmol 117(9):1216–1222
45. Yanagihara D, Watanabe S, Takagi S, Mitarai G (1993) Neuroanatomical substrate for the dorsal light response. II Effects of kainic acid-induced lesions of the valvula cerebelli on the goldfish dorsal light response Neuroscience research 16(1):33–37
46. Kaneda M, Nagashima M, Nunome T, Muramatsu T, Yamada Y, Kubo M, Muramoto K, Matsukawa T et al (2008) Changes of phospho-growth-associated protein 43 (phospho-GAP43) in the zebrafish retina after optic nerve injury: a long-term observation. Neurosci Res 61(3):281–288. https://doi.org/10.1016/j.neures.2008.03.008
47. Levy AD, Omar MH, Koleske AJ (2014) Extracellular matrix control of dendritic spine and synapse structure and plasticity in adulthood. Front Neuroanat 8:116. https://doi.org/10.3389/fnana.2014.00116
48. Emoto K (2012) Signaling mechanisms that coordinate the development and maintenance of dendritic fields. Curr Opin Neurobiol 22(5):805–811. https://doi.org/10.1016/j.conb.2012.04.005
49. Ramoa AS, Campbell G, Shatz CJ (1988) Dendritic growth and remodeling of cat retinal ganglion cells during fetal and postnatal development. J Neurosci 8(11):4239–4261
50. Maslim J, Webster M, Stone J (1986) Stages in the structural differentiation of retinal ganglion cells. J Comp Neurol 254(3):382–402. https://doi.org/10.1002/cne.902540310
51. Holt CE (1989) A single-cell analysis of early retinal ganglion cell differentiation in Xenopus: from soma to axon tip. J Neurosci 9(9):3123–3145
52. Rajan I, Cline HT (1998) Glutamate receptor activity is required for normal development of tectal cell dendrites in vivo. J Neurosci 18(19):7836–7846
53. Park KK, Liu K, Hu Y, Smith PD, Wang C, Cai B, Xu B, Connolly L et al (2008) Promoting axon regeneration in the adult CNS by modulation of the PTEN/mTOR pathway. Science 322(5903):963–966. https://doi.org/10.1126/science.1161566
54. Li X, Yang Q, Yu H, Wu L, Zhao Y, Zhang C, Yue X, Liu Z et al (2014) LIF promotes tumorigenesis and metastasis of breast cancer through the AKT-mTOR pathway. Oncotarget 5(3):788–801. https://doi.org/10.18632/oncotarget.1772
55. Ogai K, Kuwana A, Hisano S, Nagashima M, Koriyama Y, Sugitani K, Mawatari K, Nakashima H et al (2014) Upregulation of leukemia inhibitory factor (LIF) during the early stage of optic nerve regeneration in zebrafish. PLoS One 9(8):e106010. https://doi.org/10.1371/journal.pone.0106010
56. Guo X, Chandrasekaran V, Lein P, Kaplan PL, Higgins D (1999) Leukemia inhibitory factor and ciliary neurotrophic factor cause dendritic retraction in cultured rat sympathetic neurons. J Neurosci 19(6):2113–2121
57. Duchossoy Y, Horvat JC, Stettler O (2001) MMP-related gelatinase activity is strongly induced in scar tissue of injured adult spinal cord and forms pathways for ingrowing neurites. Mol Cell Neurosci 17(6):945–956. https://doi.org/10.1006/mcne.2001.0986
58. Ahmed Z, Dent RG, Leadbeater WE, Smith C, Berry M, Logan A (2005) Matrix metalloproteases: degradation of the inhibitory environment of the transected optic nerve and the scar by regenerating axons. Mol Cell Neurosci 28(1):64–78. https://doi.org/10.1016/j.mcn.2004.08.013
59. Verslegers M, Lemmens K, Van Hove I, Moons L (2013) Matrix metalloproteinase-2 and -9 as promising benefactors in development, plasticity and repair of the nervous system. Prog Neurobiol 105:60–78. https://doi.org/10.1016/j.pneurobio.2013.03.004
60. Chung SH, Awal MR, Shay J, McLoed MM, Mazur E, Gabel CV (2016) Novel DLK-independent neuronal regeneration in Caenorhabditis elegans shares links with activity-dependent ectopic outgrowth. Proc Natl Acad Sci U S A 113(20):E2852–E2860. https://doi.org/10.1073/pnas.1600564113
61. Bray ER, Noga M, Thakor K, Wang Y, Lemmon VP, Park KK, Tsoulfas P (2017) 3D visualization of individual regenerating retinal ganglion cell axons reveals surprisingly complex growth paths. eNeuro 4(4):ENEURO.0093–ENEU17.2017. https://doi.org/10.1523/ENEURO.0093-17.2017
62. Jan YN, Jan LY (2003) The control of dendrite development. Neuron 40(2):229–242
63. Li Z, Okamoto K, Hayashi Y, Sheng M (2004) The importance of dendritic mitochondria in the morphogenesis and plasticity of spines and synapses. Cell 119(6):873–887. https://doi.org/10.1016/j.cell.2004.11.003
64. Maeder CI, Shen K, Hoogenraad CC (2014) Axon and dendritic trafficking. Curr Opin Neurobiol 27:165–170. https://doi.org/10.1016/j.conb.2014.03.015
65. Bradke F, Fawcett JW, Spira ME (2012) Assembly of a new growth cone after axotomy: the precursor to axon regeneration. Nat Rev Neurosci 13(3):183–193. https://doi.org/10.1038/nrn3176

66. Karbowski J (2014) Constancy and trade-offs in the neuroanatomical and metabolic design of the cerebral cortex. Frontiers in neural circuits 8:9. https://doi.org/10.3389/fncir.2014.00009
67. Harris JJ, Jolivet R, Attwell D (2012) Synaptic energy use and supply. Neuron 75(5):762–777. https://doi.org/10.1016/j.neuron.2012.08.019
68. Zhou B, Yu P, Lin MY, Sun T, Chen Y, Sheng ZH (2016) Facilitation of axon regeneration by enhancing mitochondrial transport and rescuing energy deficits. J Cell Biol 214(1):103–119. https://doi.org/10.1083/jcb.201605101
69. Cartoni R, Pekkurnaz G, Wang C, Schwarz TL, He Z (2017) A high mitochondrial transport rate characterizes CNS neurons with high axonal regeneration capacity. PLoS One 12(9):e0184672. https://doi.org/10.1371/journal.pone.0184672
70. Scott EK, Luo L (2001) How do dendrites take their shape? Nat Neurosci 4(4):359–365. https://doi.org/10.1038/86006
71. Vandesompele J, De Preter K, Pattyn F, Poppe B, Van Roy N, De Paepe A, Speleman F (2002) Accurate normalization of real-time quantitative RT-PCR data by geometric averaging of multiple internal control genes. Genome Biol 3(7):RESEARCH0034
72. Wullimann MF, Rupp B, Reichert H (1996) Neuroanatomy of the zebrafish brain a topological atlas. https://doi.org/10.1007/978-3-0348-8979-7